Journal of Engineering Mathematics **41:** 55–73, 2001.

Non-dilatant double-shearing theory applied to granular funnel-flow in hoppers

A.J.M. SPENCER* and JAMES M. HILL
School of Mathematics and Applied Statistics, University of Wollongong, Wollongong, New South Wales 2522, Australia

Received 23 November 2000; accepted in revised form 1 May 2001

Abstract. The storage and efficient withdrawal of material from silos and hoppers is basic to numerous industrial processes. Practising engineers classify two fundamental flows, namely mass-flow and funnel-flow. The former describes the situation when the bulk solid is in motion at every point in the silo or hopper, whenever material is drawn from the outlet. The latter describes the situation when a stable channel forms, called a rat-hole, and the flow is such that only material above the rat-hole is in motion. Funnel-flow occurs whenever the outlet walls are too rough and not sufficiently steeply sloped. Funnel-flow is generally erratic and can give rise either to segregation problems or may lead to complete blockage of the outlet. Here two relevant analytical solutions of the equations for the non-dilatant double-shearing model of granular flow are presented for both plane and axially symmetric funnel-flow. These solutions give rise to flow patterns which are similar to those observed in funnel-flow in the discharge of rectangular and circular cylindrical silos and hoppers.

Key words: granular material, funnel flow, hopper flow, gravity flow.

1. Introduction

The storage of material in silos and hoppers is fundamental to many important industries such as mining, agricultural, mineral processing, pharmaceutical and numerous others arising in chemical engineering. Ideally, material discharge from a silo or hopper should be as uniform as possible, such that material is discharged in more or less the same sequence as it is loaded into the container. From a practical perspective, flows which are non-uniform, are either erratic or lead to a complete blockage, and cause serious problems. Roberts [1] provides a comprehensive account of existing developments and theory for flow of material from silos and hoppers. Jenike [2, 3] introduced the classification of two principal modes of flow which he termed mass-flow and funnel-flow and these are shown schematically in Figures 1 and 2. Mass-flow has been examined in detail by Jenike [4–6] and Johanson [7]. It is the ideal discharge mechanism because material is in motion at every point in the container whenever material is drawn from the outlet. Mass-flow guarantees complete discharge of the contents at predictable flow rates. It is a 'first-in, first-out' flow pattern and when properly designed can re-mix the material during discharge in the event that the material becomes segregated during filling. Mass-flow is usually achieved with steep smooth hopper surfaces and avoiding abrupt transitions in the walls of the container. Funnel-flow, shown in Figure 2, arises when a stable channel forms and only material above and within the channel is in motion. The channel can either be a slot in a rectangular container or a circular cavity in a cylindrical container, and

*Permanent address: Division of Theoretical Mechanics, School of Mathematical Sciences, University of Nottingham, Nottingham, NG7 2RD, UK.

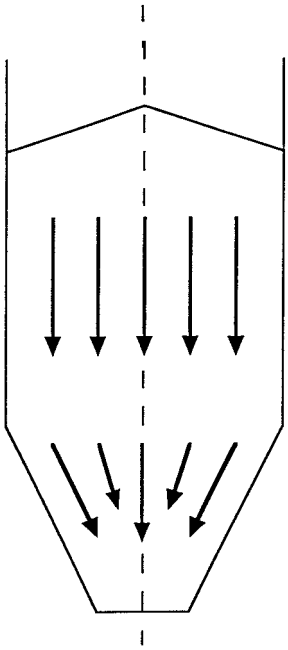

Figure 1. Mass-flow in a hopper; arrows indicate material is in motion at every point in the container.

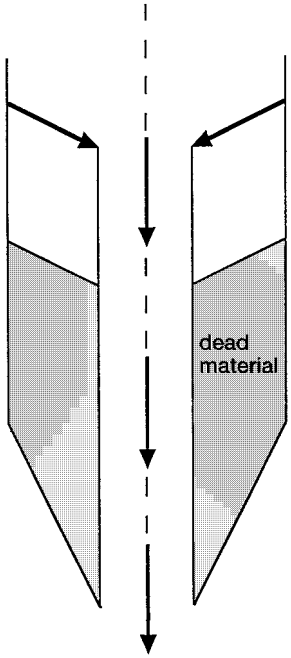

Figure 2. Funnel-flow in a hopper; arrows indicate material is flowing only from the top of the container through a central channel surrounded by a dead region.

in either case the stable channel is referred to as a rat-hole. Our purpose here is to utilize the double-shearing theory of granular flow to determine mathematical solutions which exhibit characteristics remarkably similar to those of funnel-flow inside a rat-hole.

The formulation of the equations which govern the deformation and flow of granular materials is an outstanding problem of continuum mechanics, and no single theory is widely accepted. Here we adopt the non-dilatant double-shearing theory of granular flow as originally proposed by Spencer [8] and subsequently described in more detail by Spencer [9]. In the following section we summarize the basic equations of non-dilatant double-shearing theory for both plane and axially symmetric flows. In the subsequent two sections we detail a number of exact solutions which exhibit characteristics of funnel-flow. In Section 5 of the paper we present some typical numerical results including particle flow paths.

We remark that our principal concern here is the determination of funnel-flow solutions in an existing stable rat-hole. We do not address the fundamental questions regarding conditions under which a rat-hole may form, or conditions for an existing rat-hole to be stable or unstable. These are issues which have yet to be properly addressed in the literature. Practising engineers are sceptical of classical rat-hole theory as enunciated by Jenike [2, 3] and Jenike and Yen [10, 11], which appears not to reflect actual material behaviour accurately . Hill and Cox [12] re-examine classical rat-hole theory for a vertical cylindrical cavity and present new analytical solutions for two special values of the angle of internal friction and an approximate analytical result for small angles of internal friction. However, to date a proper stability investigation of an existing rat-hole has yet to be undertaken. This is partly due to the lack of an agreed mathematical model for granular flow which involves both stress and velocity components.

Classical theory attempts to address the question of rat-hole stability without recourse to a theory involving velocity components. From a practical perspective for material flowing from a silo or hopper, the real problem is to determine the minimum diameter of the outlet such that the rat-hole is tapered (*i.e.* unstable) and this is referred to as the critical rat-hole diameter. For an unstable rat-hole, it is generally believed that the smallest compressive principal stress must exceed the unconfined yield strength of the material, which is usually denoted by f_c (see, for example, Jenike [2, 3]). Finally, we comment that Hill and Cox [13] provide analytical expressions for stress profiles for slightly tapered cylindrical granular cavities, while Spencer and Bradley [14,15] have given approximate stress and velocity solutions for gravity flow within tapering channels and tubes.

2. Basic equations of non-dilatant double-shearing theory

In this section, for quasi-static steady flow conforming to the Coulomb-Mohr yield condition, we summarize the basic equations of the double-shearing theory for granular materials for both plane and axially symmetric flows.

2.1. Plane strain flow

In terms of rectangular Cartesian coordinates (x, y, z) we consider flow in a vertical channel or slot in the (x, z) plane, with the z-axis vertically upwards. Assuming plane strain conditions, the non-zero components of the stress tensor satisfy the equilibrium equations

$$\frac{\partial \sigma_{xx}}{\partial x} + \frac{\partial \sigma_{xz}}{\partial z} = 0, \quad \frac{\partial \sigma_{xz}}{\partial x} + \frac{\partial \sigma_{zz}}{\partial z} = \rho g, \tag{2.1}$$

where ρ denotes the bulk solid density, assumed constant, and g is the acceleration due to gravity. In terms of stress invariants p and q and the stress angle ψ which are defined by

$$p = -\tfrac{1}{2}(\sigma_{xx} + \sigma_{zz}),\ q = \tfrac{1}{2}\{(\sigma_{xx} - \sigma_{zz})^2 + 4\sigma_{xz}^2\}^{1/2}, \tag{2.2}$$

$$\tan 2\psi = \frac{2\sigma_{xz}}{(\sigma_{xx} - \sigma_{zz})}, \tag{2.3}$$

we have the following standard expressions

$$\sigma_{xx} = -p + q\cos 2\psi,\ \sigma_{zz} = -p - q\cos 2\psi,\ \sigma_{xz} = q\sin 2\psi. \tag{2.4}$$

For a cohesionless granular material, the stress relations are completed with the assumption of the Coulomb–Mohr yield condition

$$q = p\sin\phi, \tag{2.5}$$

where ϕ denotes the angle of internal friction which is assumed to be constant. The above equations are generally accepted as a reasonable basis for the determination of the stress components.

The prescription of equations to determine an associated velocity profile is far more controversial. Here we assume the non-dilatant double-shearing theory. For steady flow the non-zero velocity components $u(x, z)$ and $w(x, z)$ in the x and z directions respectively, following Spencer [8, 9] satisfy the equations

$$\frac{\partial u}{\partial x} + \frac{\partial w}{\partial z} = 0, \tag{2.6}$$

$$\left(\frac{\partial u}{\partial z}+\frac{\partial w}{\partial x}\right)\cos 2\psi-\left(\frac{\partial u}{\partial x}-\frac{\partial w}{\partial z}\right)\sin 2\psi+\sin\phi\left(\frac{\partial u}{\partial z}-\frac{\partial w}{\partial x}+2\Omega\right)=0, \tag{2.7}$$

where for steady flow the quantity Ω is defined by

$$\Omega=u\frac{\partial\psi}{\partial x}+w\frac{\partial\psi}{\partial z}. \tag{2.8}$$

Equation (2.6) is the expression corresponding to the assumption that the flow is isochoric, while (2.7) expresses the condition that the flow arises as a consequence of simultaneous shearing on the two families of surfaces on which the critical shear stress is mobilized. Along with appropriate stress and velocity boundary conditions the above equations represent a complete description for quasi-static steady plane granular flow.

2.2. Axially symmetric flow

In terms of cylindrical polar coordinates (r,θ,z) we consider axially symmetric flow through a vertical circular cylindical cavity, again with the z-axis vertically upwards. In this case the non-zero components of the stress tensor satisfy the equilibrium equations

$$\frac{\partial\sigma_{rr}}{\partial r}+\frac{\partial\sigma_{rz}}{\partial z}+\frac{\sigma_{rr}-\sigma_{\theta\theta}}{r}=0,\quad \frac{\partial\sigma_{rz}}{\partial r}+\frac{\partial\sigma_{zz}}{\partial z}+\frac{\sigma_{rz}}{r}=\rho g, \tag{2.9}$$

and from the relations

$$p=-\tfrac{1}{2}(\sigma_{rr}+\sigma_{zz}),\qquad q=\tfrac{1}{2}\{(\sigma_{rr}-\sigma_{zz})^2+4\sigma_{rz}^2\}^{1/2}, \tag{2.10}$$

$$\tan 2\psi=\frac{2\sigma_{rz}}{(\sigma_{rr}-\sigma_{zz})}, \tag{2.11}$$

we may deduce

$$\sigma_{rr}=-p+q\cos 2\psi,\quad \sigma_{zz}=-p-q\cos 2\psi,\quad \sigma_{rz}=q\sin 2\psi. \tag{2.12}$$

Further, on assuming a stress state corresponding to one of the Haar-von Karman regimes, we obtain

$$\sigma_{\theta\theta}=-(p+q). \tag{2.13}$$

If $u(r,z)$ and $w(r,z)$ now denote the non-zero steady velocity components in the r and z directions, respectively, then the appropriate equations corresponding to (2.6) and (2.7) for axially symmetric flow using the non-dilatant double-shearing theory, become

$$\frac{\partial u}{\partial r}+\frac{u}{r}+\frac{\partial w}{\partial z}=0, \tag{2.14}$$

$$\left(\frac{\partial u}{\partial z}+\frac{\partial w}{\partial r}\right)\cos 2\psi-\left(\frac{\partial u}{\partial r}-\frac{\partial w}{\partial z}\right)\sin 2\psi+\sin\phi\left(\frac{\partial u}{\partial z}-\frac{\partial w}{\partial r}+2\Omega\right)=0, \tag{2.15}$$

where here for steady flow the quantity Ω is defined by

$$\Omega=u\frac{\partial\psi}{\partial r}+w\frac{\partial\psi}{\partial z}. \tag{2.16}$$

In the following two sections we present a number of solutions of these equations some of which display the characteristics of funnel-flow. We emphasize that the solutions given below are derived as steady solutions in a certain reference frame, but in the applications considered in Section 5, these solutions are exploited for motions which are not steady with respect to axes fixed in the silos. The two frames of reference differ only by a constant vertical velocity, so that in the applications context, the various arbitrary constants which emerge below must be interpreted as arbitrary functions of time.

3. Solutions for plane flow

For a cohesionless granular material, the following solution of the stress equations (2.1)–(2.5) is derived in Spencer and Bradley [10], namely

$$\begin{aligned} \sigma_{xx} &= -\rho g \ell \cot\phi, \quad \sigma_{xz} = \rho g x, \\ \sigma_{zz} &= -\frac{\rho g \ell (1+\sin^2\phi)}{\sin\phi\cos\phi} + 2\rho g \frac{(\ell^2 - x^2)^{1/2}}{\cos\phi}, \end{aligned} \tag{3.1}$$

and $\psi = \psi(x)$ is determined from

$$\tan 2\psi = \frac{x\cos\phi}{\ell\sin\phi - (\ell^2 - x^2)^{1/2}}, \tag{3.2}$$

and ℓ is a positive constant, which ensures σ_{xx} is compressive and the solution applies for $|x| \le \ell$. Now for plane steady flow with $\psi = \psi(x)$ we find from (2.6) and (2.7) on introducing the stream function $\chi(x, z)$ such that

$$u = \frac{\partial\chi}{\partial z}, \quad w = -\frac{\partial\chi}{\partial x}, \tag{3.3}$$

that $\chi(x, z)$ satisfies

$$(\cos 2\psi + \sin\phi)\frac{\partial^2\chi}{\partial z^2} - (\cos 2\psi - \sin\phi)\frac{\partial^2\chi}{\partial x^2} - 2\sin 2\psi \frac{\partial^2\chi}{\partial x\partial z} + 2\sin\phi \frac{\partial\psi}{\partial x}\frac{\partial\chi}{\partial z} = 0. \tag{3.4}$$

Again noting that $\psi = \psi(x)$, we can verify that this equation admits solutions of the form

$$\chi(x, z) = f_0(x) + z f_1(x) + z^2 f_2(x) + \cdots + z^m f_m(x), \tag{3.5}$$

where $f_j(x)$ $(j = 0, 1, 2, \ldots m)$ satisfy certain differential equations obtained by substitution of (3.5) in (3.4) and equating coefficients of z.

For example, for the case $m = 1$ we have

$$\chi(x, z) = f(x) + z g(x), \tag{3.6}$$

and (3.4) yields

$$(\cos 2\psi - \sin\phi)(f'' + z g'') + 2g' \sin 2\psi - 2g\psi' \sin\phi = 0, \tag{3.7}$$

where primes denote differentiation with respect to x. From (3.7) it is clear that $g'' = 0$ and therefore $g(x) = Ax + B$ where A and B denote arbitrary constants. Using this equation for $g(x)$, we find from (3.7) that $f(x)$ is obtained by integrating

$$(\cos 2\psi - \sin\phi) f'' + 2A \sin 2\psi - 2(Ax + B)\psi' \sin\phi = 0. \tag{3.8}$$

On using (3.2) we can show that this equation simplifies to give

$$f''(x) = \frac{2Ax}{\cos\phi(\ell^2 - x^2)^{1/2}} + \frac{\ell(Ax + B)\tan\phi}{(\ell^2 - x^2)}, \tag{3.9}$$

and one integration yields

$$\begin{aligned} f'(x) \;=\; & -\frac{2A}{\cos\phi}(\ell^2 - x^2)^{1/2} - \ell A \tan\phi \log(\ell^2 - x^2)^{1/2} \\ & + B\tan\phi \log\left(\frac{\ell + x}{\ell - x}\right)^{1/2} + C, \end{aligned} \tag{3.10}$$

where C denotes a further arbitrary constant. Altogether then, we have from (3.3), (3.6) and (3.10) the following expressions for the velocity field

$$\begin{aligned} u &= Ax + B, \\ w \;=\; & \frac{2A}{\cos\phi}(\ell^2 - x^2)^{1/2} + (A\ell - B)\tan\phi \log(\ell + x)^{1/2} \\ & + (A\ell + B)\tan\phi \log(\ell - x)^{1/2} - (Az + C). \end{aligned} \tag{3.11}$$

For the case $m = 2$ we have

$$\chi(x, z) = f(x) + zg(x) + \frac{z^2}{2}h(x), \tag{3.12}$$

and from (3.4) we obtain $h'' = 0$ and therefore $h(x) = bx + c$ and we have on equating coefficients of z and z^0,

$$\begin{aligned} g''(x) \;=\; & \frac{2bx}{\cos\phi(\ell^2 - x^2)^{1/2}} + \frac{\ell(bx + c)}{(\ell^2 - x^2)}\tan\phi, \\ f''(x) \;=\; & \frac{2xg'(x)}{\cos\phi(\ell^2 - x^2)^{1/2}} + \frac{\ell\tan\phi g(x)}{(\ell^2 - x^2)} \\ & + \frac{(bx + c)}{\cos^2\phi}\left\{1 + \sin^2\phi - \frac{2\ell\sin\phi}{(\ell^2 - x^2)^{1/2}}\right\}, \end{aligned} \tag{3.13}$$

as the two determining equations for $f(x)$ and $g(x)$, where b and c denote further arbitrary constants. These equations may be integrated formally, but we do not proceed further with the details. An application of the solution for $m = 1$ is presented in Section 5, and a possible application of the solution for $m = 2$ is mentioned in Section 6.

4. Solutions for axially symmetric flow

For a cohesionless granular material, Spencer and Bradley [14] show that a solution of (2.5), (2.9) and (2.13) having all stress components independent of z and finite along the z-axis is given by

$$\begin{aligned} \sigma_{rr} \;=\; & -\frac{\rho g r}{4\beta T}[(1 - \beta) + (1 + \beta)T^2], \qquad \sigma_{\theta\theta} = -\frac{\rho g r}{4\beta T}(1 + \beta)(1 + T^2), \\ \sigma_{zz} \;=\; & -\frac{\rho g r}{4\beta T}[(1 + \beta) + (1 - \beta)T^2], \qquad \sigma_{rz} = \frac{\rho g r}{2}, \end{aligned} \tag{4.1}$$

where here β denotes $\sin\phi$ and $T = \tan\psi$ satisfies the differential equation

$$\frac{\mathrm{d}T}{\mathrm{d}r} = \frac{T[(1-3\beta)+(1+\beta)T^2]}{r[(1-\beta)-(1+\beta)T^2]}, \tag{4.2}$$

which may be integrated to yield

$$r = \frac{r_0 T^{2n-1}}{[(1-3\beta)+(1+\beta)T^2]^n}, \tag{4.3}$$

where r_0 denotes an arbitrary constant and the index n is defined by

$$n = \frac{1-2\beta}{1-3\beta}. \tag{4.4}$$

It is clear that the character of the solution varies according as

$$0 < \beta < \tfrac{1}{3}, \quad \tfrac{1}{3} < \beta < \tfrac{1}{2}, \quad \tfrac{1}{2} < \beta < 1,$$

and $\beta = 1/3$ and $1/2$ constitute additional special cases.

For the velocity field we introduce a stream function $\chi(r, z)$ such that

$$u = \frac{1}{r}\frac{\partial\chi}{\partial z}, \quad w = -\frac{1}{r}\frac{\partial\chi}{\partial r}, \tag{4.5}$$

and then the double-shearing condition (2.15) becomes

$$(\cos 2\psi + \beta)\frac{\partial^2\chi}{\partial z^2} - (\cos 2\psi - \beta)\left(\frac{\partial^2\chi}{\partial r^2} - \frac{1}{r}\frac{\partial\chi}{\partial r}\right)$$
$$- \sin 2\psi\left(2\frac{\partial^2\chi}{\partial r\partial z} - \frac{1}{r}\frac{\partial\chi}{\partial z}\right) + 2\beta\frac{\partial\psi}{\partial r}\frac{\partial\chi}{\partial z} = 0, \tag{4.6}$$

noting again that $\beta = \sin\phi$ and that $\psi = \psi(r)$. As for plane flows, this equation admits solutions of the form

$$\chi(r, z) = f_0(r) + z f_1(r) + z^2 f_2(r) + \cdots + z^m f_m(r), \tag{4.7}$$

where $f_j(r)$ $(j = 0, 1, 2, \ldots m)$ satisfy certain differential equations obtained by substitution of (4.7) in (4.6).

For the case $m = 1$ we have

$$\chi(r, z) = f(r) + z g(r), \tag{4.8}$$

and from (4.6) we may deduce

$$g'' - \frac{g'}{r} = 0,$$

$$(\cos 2\psi - \beta)\left(f'' - \frac{f'}{r}\right) + \sin 2\psi\left(2g' - \frac{g}{r}\right) - 2\beta g\psi' = 0, \tag{4.9}$$

where primes here denote differentiation with respect to r. From $(4.9)_1$ we have

$$g(r) = A_1 r^2 + B_1, \tag{4.10}$$

Table 1. Special values of $\beta = \sin\phi$ giving rise to integer values of n as defined by (4.4).

n	-3	-2	-1	0	1	2	3
$\beta = \sin\phi$	$\frac{4}{11}$	$\frac{3}{8}$	$\frac{2}{5}$	$\frac{1}{2}$	0	$\frac{1}{4}$	$\frac{2}{7}$

where again A_1 and B_1 denote arbitrary constants, and therefore $(4.9)_2$ becomes

$$(\cos 2\psi - \beta)\left(f'' - \frac{f'}{r}\right) + \left(3A_1 r - \frac{B_1}{r}\right)\sin 2\psi - 2\beta(A_1 r^2 + B_1)\psi' = 0. \tag{4.11}$$

On writing this equation as

$$\frac{\mathrm{d}}{\mathrm{d}r}\left(\frac{f'}{r}\right) = -\left(3A_1 - \frac{B_1}{r^2}\right)\frac{\sin 2\psi}{(\cos 2\psi - \beta)} + 2\beta\frac{(A_1 r^2 + B_1)\psi'}{r(\cos 2\psi - \beta)}, \tag{4.12}$$

we can show by means of (4.2) and (4.3) that

$$\int\left(3A_1 - \frac{B_1}{r^2}\right)\frac{\sin 2\psi\,\mathrm{d}r}{(\cos 2\psi - \beta)} = \frac{3A_1 r_0}{(1-2\beta)}[(1-3\beta)s^2 + (1+\beta)]^{-n}$$
$$+\frac{2B_1}{r_0}\int[(1-3\beta)s^2 + (1+\beta)]^{n-1}\frac{\mathrm{d}s}{s}, \tag{4.13}$$

where $s = T^{-1}$. Similarly, the second integral in (4.12) can be shown to become

$$\int\left(A_1 r + \frac{B_1}{r}\right)\frac{\mathrm{d}\psi}{(\cos 2\psi - \beta)} = A_1 r_0\int\frac{s\,\mathrm{d}s}{[(1+\beta)-(1-\beta)s^2][(1+\beta)+(1-3\beta)s^2]^n}$$
$$+\frac{B_1}{r_0}\int\frac{[(1+\beta)+(1-3\beta)s^2]^n}{[(1+\beta)-(1-\beta)s^2]}\frac{\mathrm{d}s}{s}. \tag{4.14}$$

For special values of $\beta = \sin\phi$, such as those given in Table 1, n becomes a positive or negative integer which considerably facilitates the evaluation of the above integrals. In the following section we examine a special case of the above solution for the problem of axially symmetric funnel-flow.

For the case $m = 2$ we have

$$\chi(r,z) = f(r) + zg(r) + \frac{z^2}{2}h(r), \tag{4.15}$$

and from (4.6) we may deduce

$$h'' - \frac{h'}{r} = 0,$$
$$(\cos 2\psi - \beta)\left(g'' - \frac{g'}{r}\right) + \sin 2\psi\left(2h' - \frac{h}{r}\right) - 2\beta h\psi' = 0, \tag{4.16}$$
$$(\cos 2\psi - \beta)\left(f'' - \frac{f'}{r}\right) + \sin 2\psi\left(2g' - \frac{g}{r}\right) - 2\beta g\psi' - (\cos 2\psi + \beta)h = 0,$$

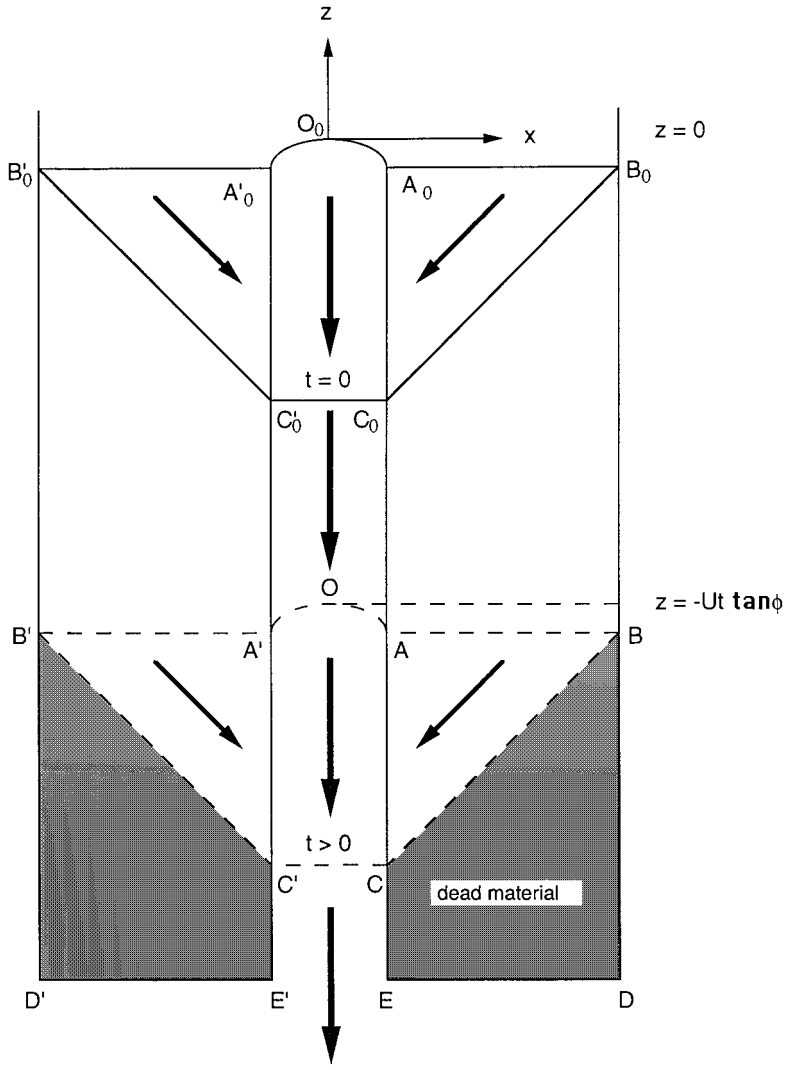

Figure 3. Idealization of funnel-flow; depicting a triangular region collapsing into a rat-hole.

which involves evaluating integrals similar to those above for $m = 1$. However, the details rapidly become complicated and we do not pursue such solutions here.

5. Applications of $m = 1$ solutions to funnel-flow

In this section we propose to model funnel-flow through a rat-hole. The model is illustrated by the configuration shown schematically in Figure 3. In this figure B_0D and B'_0D' represent the walls of the silo (which need not necessarily be straight and vertical). The origin of coordinates O is taken to be on the central axis of the rat-hole at a point which is defined later. In plane funnel flow the rat-hole is assumed to be a vertical channel bounded by the planes $x = \pm a$; these are represented in Figure 3 by A_0E and A'_0E'. The configuration is symmetrical about $x = 0$, and so it is sufficient to consider the region $x \geq 0$. Initially, at time $t = 0$, the material in the triangular region $A_0B_0C_0$ flows into the rat-hole by shear on the plane C_0B_0

with horizontal velocity component $-U$. It is assumed that C_0B_0 is at the critical slope angle ϕ and so the vertical component of velocity in $A_0B_0C_0$ is $-U\tan\phi$. The active part of the rat-hole is the region $A_0C_0C_0'A_0'$, and it is assumed that the solution described in Section 3 (with $m = 1$) is applicable in this region. The material in B_0DEC_0 is at rest and that in the lower part of the rat-hole, that is $C_0EE'C_0'$, falls vertically under gravity, provided that the gravitational force on this material exceeds the frictional forces applied across the surfaces C_0E and $C_0'E'$.

Subsequently, the interface between the moving wedge and the dead material translates downwards, so that at time $t > 0$ the wedge occupies the region ABC and the material that was initially in A_0B_0BA has flowed into or through the funnel. The surface of the material in the silo is now AB, and conservation of volume requires that the surface translates downwards with speed $U\tan\phi$, and so, if U is constant

$$A_0A = B_0B = C_0C = Ut\tan\phi. \tag{5.1}$$

At time t the active part of the rat-hole is now $A'AC'C$, and the solution described in Section 3 applies in this region .The material in $BDEC$ is 'dead', and that in $CEE'C'$ falls under gravity through the rat-hole. It is important to note that, relative to axes fixed in the silo, the motion described is not a steady motion. It is steady relative to a frame of reference that translates in the negative z direction with speed $U\tan\phi$.

A similar flow field is assumed in the case of cylindrical funnel flow, with the rat-hole being represented by a circular cylinder bounded by $r = a$. In this case a rather more complicated flow is required in the feeder region analogous to ABC, which we shall not consider here, but it is still assumed that the material shears on itself on the surface BC, and that this surface translates downwards with constant speed $U\tan\phi$.

5.1. Plane funnel-flow

With the configuration described above and illustrated in Figure 3, the boundary conditions on the velocity are the symmetry condition $u(0, z) = 0$, and for $t > 0$, the condition at the surface of the rat-hole

$$u(a, z) = -U \text{ on } AC,\ u(a, z) = 0 \text{ on } CE. \tag{5.2}$$

Hence, on assuming the solution obtained in Section 3 for the region $A'ACC'$, we find from (3.11) and (5.2) that $A = -U/a$ and $B = 0$, and therefore

$$u = -U\frac{x}{a},$$

$$w = -\frac{U}{a}\left\{l\tan\phi\log(l^2 - x^2)^{\frac{1}{2}} + 2\sec\phi(l^2 - x^2)^{\frac{1}{2}} - z\right\} - C, \tag{5.3}$$

where C here denotes a further arbitrary constant. Now for the stress boundary conditions, symmetry about the $z-$axis implies that $\sigma_{xz} = 0$ at $x = 0$, which is satisfied automatically in view of $(2.4)_3$ and (3.2). We further require that the material should shear on itself along $x = \pm a$, so that along these surfaces the maximum shear stress is mobilised and therefore on $x = a$ we require

$$\frac{\sigma_{xz}}{\sigma_{xx}} = -\tan\phi,$$

which on using (2.4) and (2.5) gives

$$\psi(a) = \tfrac{1}{4}\pi - \tfrac{1}{2}\phi, \tag{5.4}$$

and it follows that the constant ℓ in the solution (3.1) is a, the rat-hole half-width. Thus the stress field in this region is completely prescribed by (3.1) and (3.2) and the velocity field is given by (5.3) with $\ell = a$. It is not possible in this model to prescribe pointwise traction conditions on the free surface $A_0' O_0 A_0$, but by equilibrium there is zero resultant force on this surface.

To analyse the velocity field (5.3) it is convenient to introduce dimensionless variables

$$\overline{u} = \frac{u}{U}, \quad \overline{w} = \frac{w}{U}, \quad \overline{x} = \frac{x}{a}, \quad \overline{z} = \frac{z}{a}, \quad \overline{\chi} = \frac{\chi}{Ua}, \quad \overline{t} = \frac{Ut}{a}. \tag{5.5}$$

In terms of these variables the velocity field (5.3) takes the form

$$\overline{u} = -\overline{x},$$

$$\overline{w} = -\tan\phi \log(1-\overline{x}^2)^{\frac{1}{2}} - 2\sec\phi(1-\overline{x}^2)^{\frac{1}{2}} + \overline{z} + W(\overline{t}), \tag{5.6}$$

where $W(\overline{t})$ represents a time-dependent velocity. We now fix the origin of coordinates O by specifying that $w = 0$ at $z = 0$ when $t = 0$. Hence we require $W(0) = 2\sec\phi$, and since the flow field translates in the negative z direction with speed $U\tan\phi$, we have

$$W(\overline{t}) = \overline{t}\ \tan\ \phi + 2\ \sec\ \phi, \tag{5.7}$$

and hence, from (5.6)

$$\overline{w} = -\tan\phi \log(1-\overline{x}^2)^{\frac{1}{2}} - 2\ \sec\ \phi\{(1-\overline{x}^2)^{\frac{1}{2}} - 1\} + \overline{z} + \overline{t}\tan\phi. \tag{5.8}$$

The variation of $\overline{w}$ with $\overline{x}$ at $\overline{z} = 0$ and time $\overline{t} = 0$ is shown in Figure 4. We note that $\overline{w}$ has a logarithmic singularity at $\overline{x} = 1$, but that the logarithm term in (5.8) has a significant effect only in a small region adjacent to $\overline{x} = 1$. The velocity profiles for other values of $\overline{z}$ and $\overline{t}$ differ from the one shown in Figure 4 only by the superposition of a velocity of magnitude $\overline{z} + \overline{t}\tan\phi$.

The non-dimensional velocity components $\overline{u}$ and $\overline{w}$ are related to the non-dimensional stream function $\overline{\chi}$ by

$$\overline{u} = \frac{\partial\overline{\chi}}{\partial\overline{z}}, \quad \overline{w} = -\frac{\partial\overline{\chi}}{\partial\overline{x}}, \tag{5.9}$$

and it follows from (5.6), (5.8) and (5.9) that

$$\begin{aligned}\overline{\chi} \ = \ & \tfrac{1}{2}\tan\phi\,\{(1+\overline{x})\log(1+\overline{x}) - (1-\overline{x})\log(1-\overline{x}) - 2\overline{x}\} \\ & + \sec\phi\{\sin^{-1}\overline{x} + \overline{x}(1-\overline{x}^2)^{\frac{1}{2}} - 2\overline{x}\} - \overline{x}\left\{\overline{z} + \overline{t}\tan\phi\right\},\end{aligned} \tag{5.10}$$

in which an integration constant has been chosen so that $\overline{\chi} = 0$ when $\overline{x} = 0$, $\overline{z} = 0$ and $\overline{t} = 0$. The streamlines (trajectories of the velocity vector) at a given time $\overline{t}$ are the curves $\overline{\chi} = \overline{\chi}_0$, where $\overline{\chi}_0$ is constant, and hence $\overline{\chi}_0 = 0$ corresponds to the streamline $A_0' O_0 A_0$ through $\overline{x} = 0$, $\overline{z} = 0$ (the origin O_0 in Figure 3) at $\overline{t} = 0$. Since there is no flux across a streamline, there is no flow across $A_0' O_0 A_0$ at $\overline{t} = 0$, or in general across $A'A$ at time $\overline{t}$, and

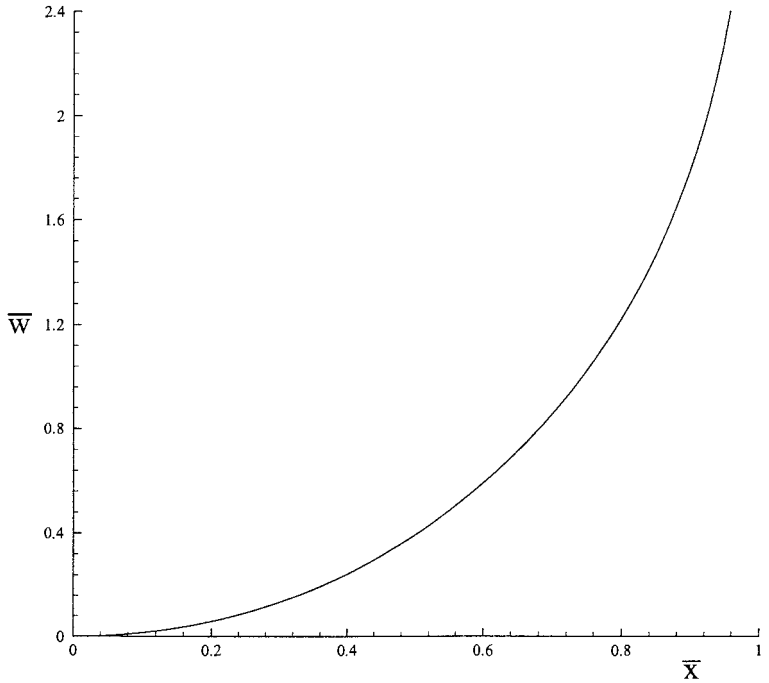

Figure 4. Magnitude of the non-dimensional downwards vertical velocity $\overline{w}(\overline{x}, 0)$ along $\overline{z} = 0$ and at time $\overline{t} = 0$ as determined from (5.8) with $\phi = \pi/6$.

so the funnel is fed solely by flow of material across AC and $A'C'$. From (5.10) the equations of the streamlines can be written as

$$\overline{z} = -\frac{\overline{\chi}_0}{\overline{x}} - \overline{t}\tan\phi + \tfrac{1}{2}\tan\phi\left\{(\overline{x}^{-1}+1)\log(1+\overline{x}) - (\overline{x}^{-1}-1)\log(1-\overline{x}) - 2\right\} + \sec\phi\left\{\overline{x}^{-1}\sin^{-1}\overline{x} + (1-\overline{x}^2)^{\frac{1}{2}} - 2\right\}. \tag{5.11}$$

Clearly if $\overline{\chi}_0 > 0$, then $\overline{z} \to -\infty$ as $\overline{x} \to 0$, and if $\overline{\chi}_0 < 0$, then $\overline{z} \to \infty$ as $\overline{x} \to 0$. Hence each of the streamlines parametrized by positive $\overline{\chi}_0$ is asymptotic to the negative $\overline{z}$ axis, and each streamline corresponding to negative $\overline{\chi}_0$ is asymptotic to the positive $\overline{z}$ axis. The upward- flowing streamlines are not relevant to the present problem, and so we consider that $\overline{\chi}_0 \geq 0$. The streamline defined by $\overline{\chi}_0 = 0$ thus forms a natural boundary to the flow field; however, it is not suggested that it necessarily forms the actual material surface, because zero traction boundary conditions are not satisfied on it. This streamline has zero slope at $\overline{x} = 0$; it intersects the $\overline{z}$ axis at $\overline{z} = 0$ and the channel walls $\overline{x} = \pm 1$ (the points A_0' and A_0 in Figure 3) at $\overline{z} = \tan\phi(\log 2 - 1) - (2 - \frac{\pi}{2})\sec\phi$. The field of streamlines at $\overline{t} = 0$ is shown in Figure 5 for $\phi = \pi/6$. The numbers on the streamlines denote values of $\overline{\chi}_0$ on the streamlines. At subsequent times the field is translated in the negative $\overline{z}$ direction without distortion by an amount $\overline{t}\tan\phi$.

Because the motion is not steady the particle paths do not coincide with the streamlines. The particle paths are given parametrically by the equations

$$\frac{\mathrm{d}\overline{x}}{\mathrm{d}\overline{t}} = \overline{u}(\overline{x}, \overline{z}, \overline{t}), \quad \frac{\mathrm{d}\overline{z}}{\mathrm{d}\overline{t}} = \overline{w}(\overline{x}, \overline{z}, \overline{t}). \tag{5.12}$$

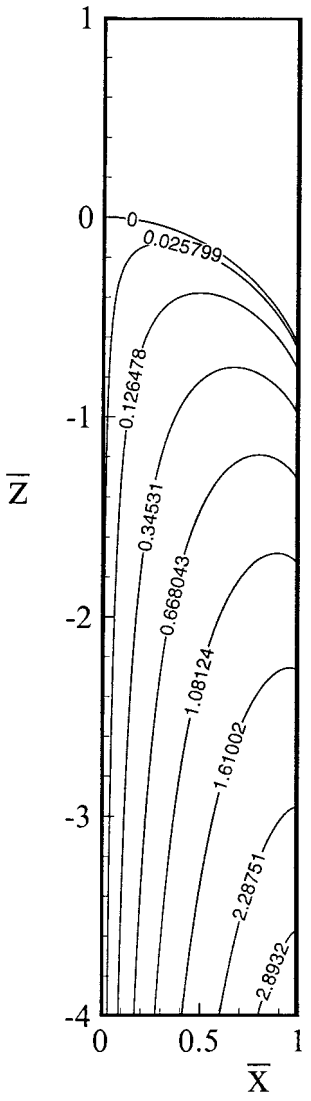

Figure 5. Streamlines for the velocity field $(5.6)_1$ and (5.8) as calculated from the stream function (5.10) with $\bar{t} = 0$ and $\phi = \pi/6$.

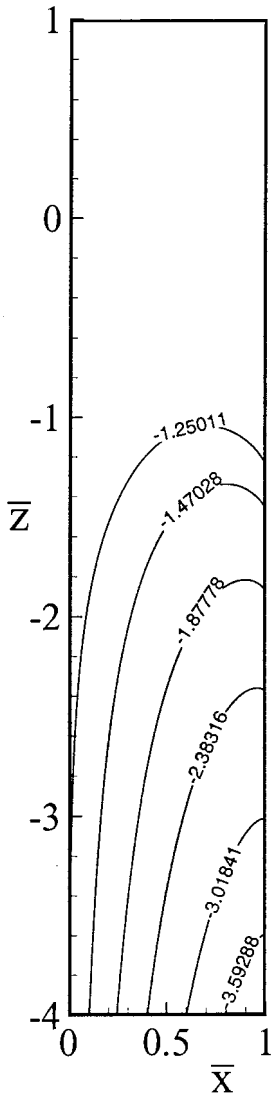

Figure 6. Particle paths which cross $\bar{x} = 1$ at time $\bar{t} = 0$ as determined from (5.18) for $\phi = \pi/6$.

Hence, from (5.6) and (5.12)

$$\frac{\mathrm{d}\bar{x}}{\mathrm{d}\bar{t}} = -\bar{x},$$

and therefore

$$\bar{x} = \bar{X}e^{-\bar{t}}, \quad \bar{t} = -\log(\bar{x}/\bar{X}), \tag{5.13}$$

where $(\bar{X}, \bar{Z})$ denote the dimensionless coordinates at $\bar{t} = 0$ of the particle which has scaled coordinates $(\bar{x}, \bar{z})$ at time $\bar{t}$.

Now from (5.8) and $(5.12)_2$ we have

$$\frac{\mathrm{d}\overline{z}}{\mathrm{d}\overline{t}} = \overline{z} + \overline{t}\tan\phi - \tan\phi\log(1-\overline{x}^2)^{\frac{1}{2}} - 2\sec\phi\left\{(1-\overline{x}^2)^{\frac{1}{2}} - 1\right\}, \tag{5.14}$$

and by substituting for $\overline{t}$ from $(5.13)_2$ in (5.14) and noting that $\mathrm{d}\overline{z}/\mathrm{d}\overline{t} = -\overline{x}\mathrm{d}\overline{z}/\mathrm{d}\overline{x}$ there follows

$$\overline{x}\frac{\mathrm{d}\overline{z}}{\mathrm{d}\overline{x}} = -\overline{z} + \tan\phi\log(\overline{x}/\overline{X}) + \tan\phi\log(1-\overline{x}^2)^{\frac{1}{2}} + 2\sec\phi\left\{(1-\overline{x}^2)^{\frac{1}{2}} - 1\right\},$$

and hence

$$\begin{aligned}\overline{x}\ \overline{z} \ &= \int\left[\tan\phi\left\{\log(\overline{x}/\overline{X}) + \log(1-\overline{x}^2)^{\frac{1}{2}}\right\} + 2\sec\phi\left\{(1-\overline{x}^2)^{\frac{1}{2}} - 1\right\}\right]\mathrm{d}\overline{x} + K\\ &= \tan\phi\left\{\overline{x}\log(\overline{x}/\overline{X}) + \frac{1}{2}(1+\overline{x})\log(1+\overline{x}) - \frac{1}{2}(1-\overline{x})\log(1-\overline{x}) - 2\overline{x}\right\}\\ &\quad + \sec\phi\left\{\sin^{-1}\overline{x} + \overline{x}(1-\overline{x}^2)^{\frac{1}{2}} - 2\overline{x}\right\} + K,\end{aligned} \tag{5.15}$$

where K is constant on a particle path. Since $\overline{z} = \overline{Z}$ when $\overline{x} = \overline{X}$

$$\begin{aligned}\overline{X}\ \overline{Z} \ &= \tan\phi\left\{\frac{1}{2}(1+\overline{X})\log(1+\overline{X}) - \frac{1}{2}(1-\overline{X})\log(1-\overline{X}) - 2\overline{X}\right\}\\ &\quad + \sec\phi\left\{\sin^{-1}\overline{X} + \overline{X}(1-\overline{X}^2)^{\frac{1}{2}} - 2\overline{X}\right\} + K.\end{aligned} \tag{5.16}$$

Hence, by eliminating K from (5.15) and (5.16), and simplifying, we obtain the equations of the particle paths:

$$\begin{aligned}\overline{z} \ &= \frac{\overline{X}\ \overline{Z}}{\overline{x}} + \tan\phi\left\{\log\left(\frac{\overline{x}}{\overline{X}}\right) + \frac{1}{2}\left(\frac{1}{\overline{x}}+1\right)\log(1+\overline{x}) - \frac{1}{2}\left(\frac{1}{\overline{x}}-1\right)\log(1-\overline{x})\right.\\ &\quad \left. -\frac{1}{2}\left(\frac{1}{\overline{x}}+\frac{\overline{X}}{\overline{x}}\right)\log(1+\overline{X}) + \frac{1}{2}\left(\frac{1}{\overline{x}}-\frac{\overline{X}}{\overline{x}}\right)\log(1-\overline{X}) - 2\left(1-\frac{\overline{X}}{\overline{x}}\right)\right\}\\ &\quad + \sec\phi\left\{\frac{\sin^{-1}\overline{x}}{\overline{x}} - \frac{\sin^{-1}\overline{X}}{\overline{x}} + (1-\overline{x}^2)^{\frac{1}{2}} - \frac{\overline{X}}{\overline{x}}(1-\overline{X}^2)^{\frac{1}{2}} - 2(1-\frac{\overline{X}}{\overline{x}})\right\}.\end{aligned} \tag{5.17}$$

The paths of the particles which enter the rat-hole across $\overline{x} = 1$ at time $\overline{t} = 0$ follow by setting $\overline{X} = 1$ in (5.17) which gives

$$\begin{aligned}\overline{z} \ &= \frac{\overline{Z}}{\overline{x}} + \tan\phi\left\{\log\overline{x} + \frac{1}{2}\left(\frac{1}{\overline{x}}+1\right)\log(1+\overline{x}) - \frac{1}{2}\left(\frac{1}{\overline{x}}-1\right)\log(1-\overline{x})\right.\\ &\quad \left. -2\left(1-\frac{1}{\overline{x}}\right) - \frac{\log 2}{\overline{x}}\right\} + \sec\phi\left\{\frac{\sin^{-1}\overline{x}}{\overline{x}} + (1-\overline{x}^2)^{\frac{1}{2}} - \frac{\pi}{2\overline{x}} - 2(1-\frac{1}{\overline{x}})\right\}.\end{aligned} \tag{5.18}$$

The particle paths are asymptotic to the negative z-axis provided that $\overline{Z} < -(2-\log 2)\tan\phi - (2-\frac{\pi}{2})\sec\phi$. Some typical paths of particles crossing $\overline{x} = 1$ at time $\overline{t} = 0$ are shown in Figure 6, where the numerical values shown on the curves are values of $\overline{Z}$. Paths of particles crossing $\overline{x} = 1$ at subsequent times $\overline{t}$ are displaced downwards by a scaled distance $\overline{t}\tan\phi$.

5.2. AXIALLY SYMMETRIC FUNNEL-FLOW

Similarly, for axially symmetric funnel-flow, we assume the velocity boundary conditions

$$u(0,z)=0,$$

$$u(a,z)=-U \text{ on } AC, \quad u(a,z)=0 \text{ on } CE, \tag{5.19}$$

and then from the $m=1$ solution given in Section 4 we have $A_1=-U/a$ and $B_1=0$ and, in terms of dimensionless variables

$$\overline{u}=\frac{u}{U}, \quad \overline{w}=\frac{w}{U}, \quad \overline{r}=\frac{r}{a}, \quad \overline{z}=\frac{z}{a}, \quad \overline{\chi}=\frac{\chi}{Ua^2}, \quad \overline{t}=\frac{Ut}{a}, \tag{5.20}$$

the velocity field can be shown to become (provided that $\sin\phi \neq 1/2$)

$$\begin{aligned}\overline{u} &= -\overline{r},\\ \overline{w} &= \frac{-3\overline{r}T}{(1-2\sin\phi)}-2\sin\phi\int\frac{\overline{r}\,\mathrm{d}T}{(1+\sin\phi)T^2-(1-\sin\phi)}+2\overline{z}+W(\overline{t}),\end{aligned} \tag{5.21}$$

where $T=\tan\psi$ and $\overline{r}$ and T are related by (4.3) and $W(\overline{t})$ is a function of $\overline{t}$. We note that the constant r_0 is determined by the condition

$$\psi(a)=\tfrac{1}{4}\pi-\tfrac{1}{2}\phi, \tag{5.22}$$

which means that $T(a)=(1-\sin\phi)/\cos\phi$ and from (4.3) r_0 is given explicitly as

$$\frac{r_0}{a}=2^n(1-2\sin\phi)^n\left(\frac{\cos\phi}{1-\sin\phi}\right)^{2n-1}. \tag{5.23}$$

The special case $\phi=\pi/6$, $\sin\phi=1/2$ and $n=0$ can be included by a limiting process, but is more easily dealt with directly. In this case (4.3) gives $T=\tan\psi=r_0/r=1/\sqrt{3}\overline{r}$ and the stress solution (4.1) simplifies to become

$$\begin{aligned}\sigma_{rr}&=-\frac{\sqrt{3}\rho g}{4a}\left(r^2+a^2\right), \quad \sigma_{\theta\theta}=-\frac{\sqrt{3}\rho g}{4a}\left(3r^2+a^2\right),\\ \sigma_{zz}&=-\frac{\sqrt{3}\rho g}{4a}\left(3r^2+\frac{a^2}{3}\right), \quad \sigma_{rz}=\frac{\rho g r}{2},\end{aligned} \tag{5.24}$$

It then follows from (4.9) that the velocity field for $\phi=\pi/6$ is given by

$$\overline{u}=-\overline{r}, \quad \overline{w}=-\frac{1}{\sqrt{3}}\log(1-\overline{r}^2)+2\overline{z}+W_1(\overline{t}), \tag{5.25}$$

and for simplicity we consider this case. As in the plane flow case, $W_1(\overline{t})$ is determined by the requirement that $\overline{w}=0$ at $\overline{r}=0$ on the surface $\overline{z}=-\overline{t}\tan\phi=-\overline{t}/\sqrt{3}$; thus $W_1(\overline{t})=2\overline{t}/\sqrt{3}$ and hence

$$\overline{w}=-\frac{1}{\sqrt{3}}\log(1-\overline{r}^2)+2\left(\overline{z}+\frac{\overline{t}}{\sqrt{3}}\right). \tag{5.26}$$

The velocity profile at $\overline{z}=0$, $\overline{t}=0$ is shown in Figure 7. The velocity at other times is given by superposing the velocity $(\overline{z}+\overline{t}/\sqrt{3})$ on this.

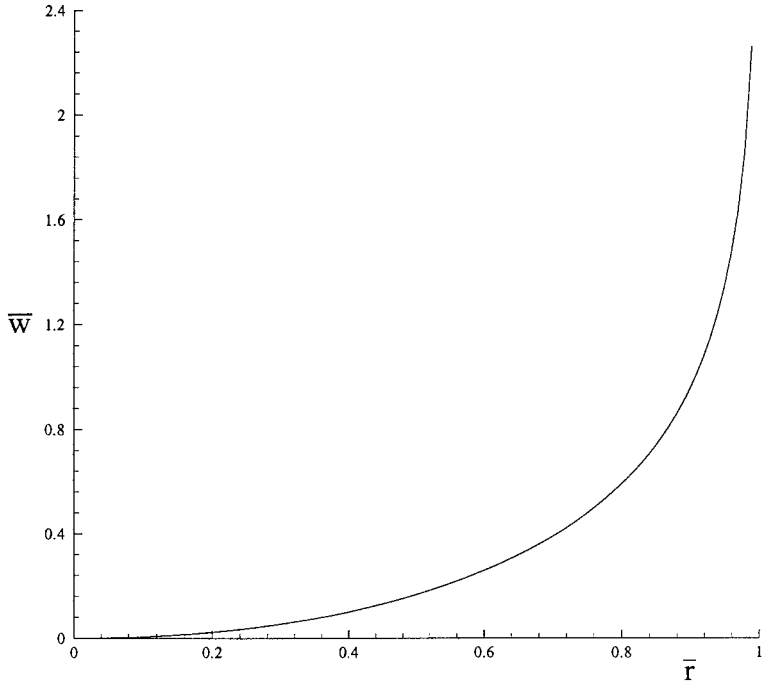

Figure 7. Magnitude of the non-dimensional downwards vertical velocity $\overline{w}(\overline{r}, 0)$ along $\overline{z} = 0$ and at time $\overline{t} = 0$ as determined from (5.26) with $\phi = \pi/6$.

The scaled velocity components are related to the scaled stream function as

$$\overline{u} = \frac{1}{\overline{r}}\frac{\partial \overline{\chi}}{\partial \overline{z}}, \quad \overline{w} = -\frac{1}{\overline{r}}\frac{\partial \overline{\chi}}{\partial \overline{r}}, \tag{5.27}$$

and hence, from (5.25) and (5.26) we have

$$\overline{\chi} = -\frac{1}{2\sqrt{3}}\left\{(1-\overline{r}^2)\log(1-\overline{r}^2) + \overline{r}^2\right\} - \overline{r}^2\left(\overline{z} + \frac{\overline{t}}{\sqrt{3}}\right), \tag{5.28}$$

where the integration constant has been chosen so that $\overline{\chi} = 0$ when $\overline{r} = 0$, $\overline{z} = 0$ and $\overline{t} = 0$, so that $\overline{\chi} = 0$ represents the streamline $A_0' O_0 A_0$ at $\overline{t} = 0$. The streamlines are the curves $\overline{\chi} = \overline{\chi}_0$ ($\overline{\chi}_0 \geq 0$) and from (5.28) they may be expressed as

$$\overline{z} = -\frac{\overline{\chi}_0}{\overline{r}^2} - \frac{\overline{t}}{\sqrt{3}} - \frac{1}{2\sqrt{3}}\left[\left(\frac{1}{\overline{r}^2} - 1\right)\log(1-\overline{r}^2) + 1\right]. \tag{5.29}$$

All of the streamlines except $\overline{\chi}_0 = 0$ are asymptotic to the negative z axis. The field of streamlines at $\overline{t} = 0$ is shown in Figure 8 where the numbers on the streamlines denote the value of $\overline{\chi}_0$ on the streamline.

The particle paths are given by

$$\frac{\mathrm{d}\overline{r}}{\mathrm{d}\overline{t}} = \overline{u}(\overline{r}, \overline{z}, \overline{t}), \quad \frac{\mathrm{d}\overline{z}}{\mathrm{d}\overline{t}} = \overline{w}(\overline{r}, \overline{z}, \overline{t}), \tag{5.30}$$

which give, from (5.25) and (5.26)

$$\frac{\mathrm{d}\overline{r}}{\mathrm{d}\overline{t}} = -\overline{r}, \quad \frac{\mathrm{d}\overline{z}}{\mathrm{d}\overline{t}} = -\frac{1}{\sqrt{3}}\log(1-\overline{r}^2) + 2\left(\overline{z} + \frac{\overline{t}}{\sqrt{3}}\right). \tag{5.31}$$

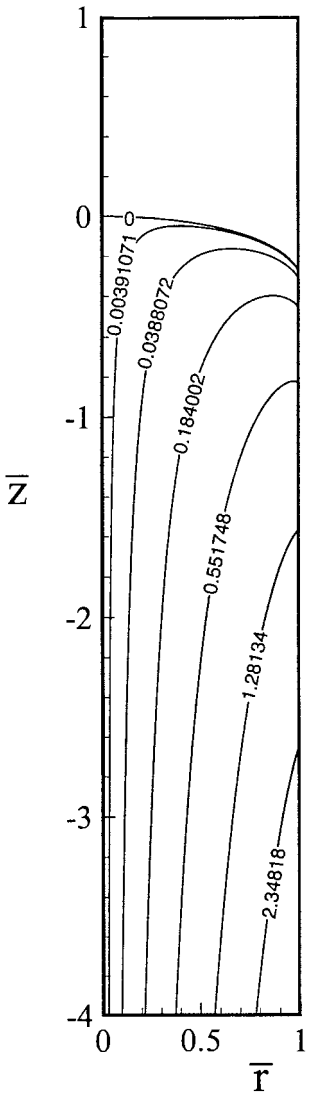

Figure 8. Streamlines for the velocity field $(5.25)_1$ and (5.26) as calculated from the stream function (5.28) with $\bar{t} = 0$ and $\phi = \pi/6$.

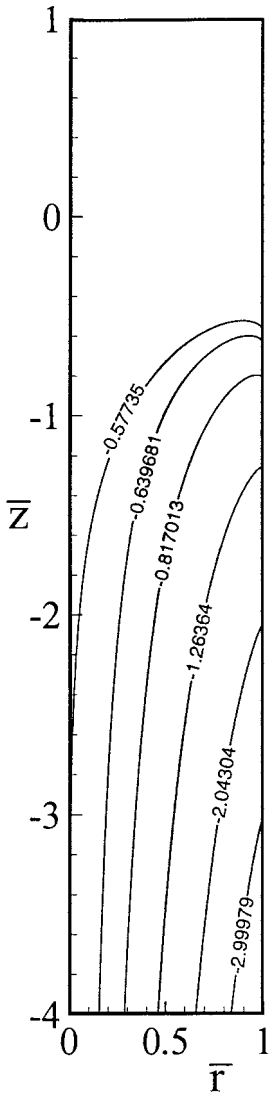

Figure 9. Particle paths which cross $\bar{r} = 1$ at time $\bar{t} = 0$ as determined from (5.33) for $\phi = \pi/6$.

These may be integrated in a manner similar to that used in the plane flow case to give

$$\begin{aligned}
\bar{r} &= \bar{R}\mathrm{e}^{-\bar{t}}, \quad \bar{t} = -\log(\bar{r}/\bar{R}), \\
\bar{z} &= \frac{\bar{R}^2\bar{Z}}{\bar{r}^2} - \frac{1}{2\sqrt{3}}\left\{\left(\frac{1}{\bar{r}^2} - 1\right)\log(1-\bar{r}^2) - \left(\frac{1}{\bar{r}^2} - \frac{\bar{R}^2}{\bar{r}^2}\right)\log(1-\bar{R}^2)\right. \\
&\quad \left. -2\log\frac{\bar{r}}{\bar{R}} - 2\left(\frac{\bar{R}^2}{\bar{r}^2} - 1\right)\right\},
\end{aligned} \tag{5.32}$$

where $(\overline{R}, \overline{Z})$ is the position at $\overline{t} = 0$ of the particle that occupies $(\overline{r}, \overline{z})$ at time $\overline{t}$. In particular the paths of particles that are on the edge $\overline{r} = 1$ of the rat-hole at $\overline{t} = 0$ are given by

$$\overline{z} = \frac{\overline{Z}}{\overline{r}^2} - \frac{1}{2\sqrt{3}} \left\{ \left(\frac{1}{\overline{r}^2} - 1 \right) \log(1 - \overline{r}^2) - 2 \log \overline{r} - 2 \left(\frac{1}{\overline{r}^2} - 1 \right) \right\}. \tag{5.33}$$

Some of these particle paths are shown in Figure 9, where the numerical values shown on the curves are values of $\overline{Z}$. They are asymptotic to the negative z axis for all $\overline{Z} < -1/\sqrt{3}$.

6. Conclusions

For the most part the results described in section 5 are plausible and qualitatively are reasonably consistent with the observed behaviour of granular materials in funnel flow. There are however a few questions that require some discussion.

Firstly, the fields of streamlines and particle paths do not conform to expected behaviour in the neighbourhood of the upper surface $z = -Ut \tan \phi$ of the rat-hole, in that in this region there is a small upward component of the motion close to the funnel walls. The probable reason for this is that the model does not admit satisfaction of stress boundary conditions at the free surface. This surface is necessarily a streamline, but the stress solutions (3.1) and (5.24) imply that the streamlines $\overline{\chi}_0 = 0$ are subject to a variable vertical pressure, as well as a shear tractions, and these forces must be applied in order to maintain the given velocity solutions. The natural way to apply these normal pressures is by a surcharge of granular material, but such a surcharge in turn affects the flow field. It follows therefore that the model cannot be expected to give good results in the neighbourhood of the free surface. This does not preclude its applicability at depths well below this surface. A more refined model might involve a boundary layer solution close to the surface, but this would involve constructing the shape of the free surface and probably require including regions in the body in which the stress is below yield and which move as rigid bodies. Such an analysis would be very difficult, even as a numerical exercise. Similar considerations apply to the transition region in the neighbourhood of $C'C$ in Figure 3, at the base of the active part of the rat-hole.

Another difficulty is the prediction of logarithmic singularities in the vertical velocity component at the boundary of the rat-hole. These predict infinite upward velocity at $x = a$ and $r = a$, which is clearly unrealistic. However the singularity is weak, affects only a small region near the boundary of the rat-hole, and is hardly noticeable on the scale of Figures 5–6 and 8–9. There is no discontinuity in the streamlines or particle paths. The singularity in the model may be due to neglect of effects such as dilatancy, finite grain size and inertia, as well as the idealised geometry, and is probably not reflected in the behaviour of real granular materials.

Despite these limitations, the model seems to be capable of capturing many of the features of funnel-flow in silos and hoppers. It has been shown that, away from the free surface, some exact solutions of the equations of the non-dilatant double-shearing theory for granular materials give flow patterns that are similar to those observed in funnel-flow in the discharge of rectangular and circular cylindrical silos and hoppers. Although the theory employed is a simple one, and cannot reflect all the complexities of behaviour of real granular materials, it appears to go some way towards describing the funnel-flow phenomenon.

In this paper we have only considered in detail the case $m = 1$ of (3.5) and (4.7). In this case the horizontal velocity component is independent of the coordinate z, which seems

appropriate for a silo with vertical walls, such as is shown in Figure 3. The case $m = 2$ gives horizontal velocity components that vary linearly with z, which may be a better model for funnel flow in wedge-shaped or conical silos, but this case has not been investigated in detail.

Acknowledgements

This work is sponsored by the Australian Research Council, both through the Large Grant Scheme and the provision of a Senior Research Fellowship for JMH. The work of AJMS was also made possible by the award of a Royal Society Study Visit Grant. The authors gratefully acknowledge this support. The authors also wish to express their gratitude to Professor Peter Arnold for numerous stimulating discussions on this problem and related topics and to Grant Cox for undertaking the numerical work.

References

1. A.W. Roberts, Bulk solids handling: Recent developments and future directions. *Bulk Solids Handling* 11 (1991) 17–35.
2. A.W. Jenike, Gravity flow of bulk solids. Utah Engineering Experiment Station Bulletin No. 108 (1962).
3. A.W. Jenike, Gravity flow of solids. *Trans. Inst. Chem. Engineers* 40 (1962) 264–274.
4. A.W. Jenike, Storage and flow of solids. Utah Engineering Experiment Station Bulletin No. 123 (1964).
5. A.W. Jenike, Steady gravity flow of frictional-cohesive solids in converging channels. *J. Appl. Mech.* 31 (1964) 5–11.
6. A.W. Jenike, Gravity flow of frictional-cohesive solids-convergence to radial stress fields. J. Appl. Mech. 32 (1965) 205–207.
7. J.R. Johanson, Stress and velocity fields in the gravity flow of bulk solids. *J. Appl. Mech.* 31 (1964) 499–506.
8. A.J.M. Spencer, A theory of the kinematics of ideal soils under plane strain conditions. *J. Mech. Phy. Solids* 12 (1964) 337–351.
9. A.J.M. Spencer, Deformation of ideal granular materials. In: *Mechanics of Solids*, H.G. Hopkins and M. J. Sewell (eds), Oxford, (Pergamon Press,1982) pp. 607–652.
10. A.W. Jenike and B.C. Yen, Slope stability in axial symmetry. Utah Engineering Experiment Station Bulletin No. 115 (1962).
11. A.W. Jenike and B.C. Yen, Slope stability in axial symmetry. In: *Proc. 5th Symposium on Rock Mechanics*, University of Minnesota, May 1962 (Pergamon Press, 1963) pp. 689–711.
12. J.M. Hill and G.M. Cox, Granular cylindrical cavities and classical rat-hole theory. *Int. J. Num. Anal. Methods Geomechanics* 24 (2000) 971–990.
13. J.M. Hill and G.M. Cox, Stress profiles for tapered cylindrical granular cavities, *Int. J. Solids Structures* 38 (2001) 3795–3811.
14. A.J.M. Spencer and N.J. Bradley, Gravity flow of a granular material in compression between vertical walls and through a tapering vertical channel. *Q. Jl. Mech. Appl. Math.* 45 (1992) 733–746.
15. A.J.M. Spencer and N.J. Bradley, Gravity flow of granular materials in contracting cylinders and tapered tubes. *Int. J. Engng. Sci.*, submitted for publication.